UC San Diego

UC San Diego Previously Published Works

Title

A Genome-Wide CRISPR-Cas9 Screen Reveals the Requirement of Host Cell Sulfation for Schmallenberg Virus Infection.

Permalink

Journal

Authors

Thamamongood, Thiprampai
Aebischer, Andrea
Wagner, Valentina
et al.

Publication Date

DOI

Peer reviewed

A Genome-Wide CRISPR-Cas9 Screen Reveals the Requirement of Host Cell Sulfation for Schmallenberg Virus Infection

Thiprampai Thamamongood,[a,b,c,d] Andrea Aebischer,[e] Valentina Wagner,[a,b] Max W. Chang,[f] Roland Elling,[g,h] Christopher Benner,[f] Adolfo García-Sastre,[i,j,k,l] Georg Kochs,[a,b] Martin Beer,[e] Martin Schwemmle[a,b]

[a]Institute of Virology, Medical Center-University of Freiburg, Freiburg, Germany
[b]Faculty of Medicine, University of Freiburg, Freiburg, Germany
[c]Spemann Graduate School of Biology and Medicine, University of Freiburg, Freiburg, Germany
[d]Faculty of Biology, University of Freiburg, Freiburg, Germany
[e]Institute of Diagnostic Virology, Friedrich-Loeffler-Institut, Greifswald-Insel Riems, Germany
[f]Department of Medicine, University of California, San Diego, San Diego, California, USA
[g]Department of Pediatrics and Adolescent Medicine, Medical Center-University of Freiburg, Freiburg, Germany
[h]Institute for Immunodeficiency, Center for Chronic Immunodeficiency, Medical Center-University of Freiburg, Faculty of Medicine, University of Freiburg, Freiburg, Germany
[i]Department of Microbiology, Icahn School of Medicine at Mount Sinai, New York, New York, USA
[j]Global Health and Emerging Pathogens Institute, Icahn School of Medicine at Mount Sinai, New York, New York, USA
[k]Department of Medicine, Division of Infectious Diseases, Icahn School of Medicine at Mount Sinai, New York, New York, USA
[l]The Tisch Cancer Institute, Icahn School of Medicine at Mount Sinai, New York, New York, USA

ABSTRACT Schmallenberg virus (SBV) is an insect-transmitted orthobunyavirus that can cause abortions and congenital malformations in the offspring of ruminants. Even though the two viral surface glycoproteins Gn and Gc are involved in host cell entry, the specific cellular receptors of SBV are currently unknown. Using genome-wide CRISPR-Cas9 forward screening, we identified 3′-phosphoadenosine 5′-phosphosulfate (PAPS) transporter 1 (PAPST1) as an essential factor for SBV infection. PAPST1 is a sulfotransferase involved in heparan sulfate proteoglycan synthesis encoded by the solute carrier family 35 member B2 gene (*SLC35B2*). SBV cell surface attachment and entry were largely reduced upon the knockout of *SLC35B2*, whereas the reconstitution of *SLC35B2* in these cells fully restored their susceptibility to SBV infection. Furthermore, treatment of cells with heparinase diminished infection with SBV, confirming that heparan sulfate plays an important role in cell attachment and entry, although to various degrees, heparan sulfate was also found to be important to initiate infection by two other bunyaviruses, La Crosse virus and Rift Valley fever virus. Thus, PAPST1-triggered synthesis of cell surface heparan sulfate is required for the efficient replication of SBV and other bunyaviruses.

IMPORTANCE SBV is a newly emerging orthobunyavirus (family *Peribunyaviridae*) that has spread rapidly across Europe since 2011, resulting in substantial economic losses in livestock farming. In this study, we performed unbiased genome-wide CRISPR-Cas9 screening and identified PAPST1, a sulfotransferase encoded by *SLC35B2*, as a host entry factor for SBV. Consistent with its role in the synthesis of heparan sulfate, we show that this activity is required for efficient infection by SBV. A comparable dependency on heparan sulfate was also observed for La Crosse virus and Rift Valley fever virus, highlighting the importance of heparan sulfate for host cell infection by bunyaviruses. Thus, the present work provides crucial insights into virus-host interactions of important animal and human pathogens.

KEYWORDS CRISPR-Cas, orthobunyavirus, Schmallenberg virus, host entry factor

Schmallenberg virus (SBV), an orthobunyavirus from the family *Peribunyaviridae*, was first identified in 2011 in cattle from a farm near the city of Schmallenberg (North Rhine-Westphalia, Germany) (1) and has since spread rapidly, causing a large epidemic in European livestock. SBV is transmitted by midges from the *Culicoides* species (2, 3), predominately infects ruminants, and causes only mild clinical signs in adult animals. However, infection of pregnant animals during a critical period of pregnancy can induce severe congenital malformations, abortions, or stillbirth (4, 5).

The family *Peribunyaviridae* belongs to the order *Bunyavirales* (6). Among *Bunyavirales*, several viruses, including La Crosse virus (LACV), hantavirus, Rift Valley fever virus (RVFV), Crimean-Congo hemorrhagic fever virus (CHHFV), and severe fever with thrombocytopenia syndrome virus (SFTSV), are vector transmitted and can cause zoonotic diseases with high mortality rates (7–11). Orthobunyaviruses have a tripartite single-stranded negative-sense RNA genome consisting of the large (L), medium (M), and small (S) segments. The L segment encodes the RNA-dependent RNA polymerase (RdRp), which is responsible for viral transcription and replication. The S segment encodes the nucleoprotein (N), which encapsidates the viral genome, as well as the nonstructural protein NSs, which is known to interfere with host innate immunity (12, 13). The M segment encodes the two viral surface glycoproteins Gn and Gc and the nonstructural protein NSm. Gc is predicted to be a class II membrane fusion protein with the fusion peptide located within the conserved, membrane-proximal, C-terminal core region (14). The N-terminal variable part of Gc forms trimeric spikes protruding from the viral membrane (3). Studies with LACV suggest that Gc plays a crucial role in viral attachment in both insect and mammalian cells. In contrast, Gn might function as an additional attachment protein exclusively in mosquito cells (15–18).

At present, potential cell surface receptors recognized by the surface glycoproteins of SBV and other orthobunyaviruses remain poorly characterized. However, a recent study reported that heparan sulfate (HS) proteoglycan is an important attachment factor for SBV (19). In the present study, we confirmed this finding by an unbiased genome-wide CRISPR-Cas9 screening approach for cellular factors required for mammalian cell entry of SBV and additionally other bunyaviruses. This technique has been used previously to uncover host factors involved in viral entry, e.g., for bat influenza A-like viruses of the H17N10 and H18N11 subtypes, human immunodeficiency virus (HIV), chikungunya virus (CHIKV), adeno-associated virus (AAV), dengue virus, hepatitis C virus (HCV), and Zika virus (ZKV) (20–26).

RESULTS

Identification of a PAPST1 sulfate transporter as an entry factor for SBV. To identify host factors involved in SBV entry, we performed a genome-wide CRISPR-Cas9-based screen in SBV-susceptible 293T cells (Fig. 1A). For this purpose, we generated a 293T cell clone expressing Cas9 (293T-Cas9). Next, we transduced these cells with a lentiviral single guide RNA (sgRNA) library targeting 19,114 genes (4 sgRNAs/gene) and 1,000 nontargeting control sgRNAs (Brunello library) (27) at a multiplicity of infection (MOI) of 0.3 to ensure that each cell expresses only one sgRNA. The transduced 293T-Cas9 cells were selected with puromycin for 10 days and subsequently expanded to achieve 1,000-fold coverage for each sgRNA in the cell pool (approximately 8.0×10^8 cells). We then infected these cells with SBV isolate BH80 at an MOI of 0.1 and harvested mock-infected cells in parallel. After 3 rounds of infection to ensure that selected survivors were resistant to SBV, genomic DNA (gDNA) of survivor cells was collected and subjected to Illumina sequencing to determine the enrichment of the integrated sgRNAs using the MAGeCK suite (28) (Fig. 1B). The top-hit candidate of this analysis was the solute carrier family 35 member B2 gene (*SLC35B2*), encoding 3′-phosphoadenosine 5′-phosphosulfate (PAPS) transporter 1 (PAPST1), involved in HS proteoglycan synthesis (29). Since the sulfation of mammalian cell surface proteins depends on the Golgi-resident sulfotransferase PAPST1 (30), we postulated that HS might be crucial for the cellular entry of SBV. Besides *SLC35B2*, the olfactory receptor family 5 subfamily P
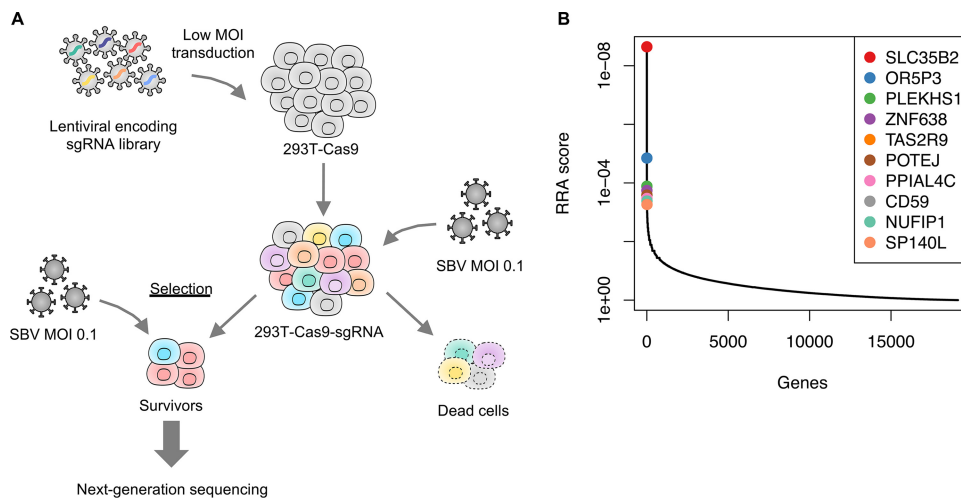
FIG 1 Identification of a sulfate transporter as an entry factor for SBV. (A) Schematic overview of the genome-wide CRISPR-Cas9 screen. 293T cells stably expressing Cas9 (293T-Cas9) were transduced with lentiviruses encoding a human CRISPR knockout pooled sgRNA library at an MOI of 0.3. At 2 days posttransduction, cells (293T-Cas9-sgRNA) were selected with puromycin (1 μg/ml) for 10 days and subsequently infected with SBV at an MOI of 0.1. Survivors were reinfected with SBV at an MOI of 0.1 for 2 more rounds and harvested to isolate genomic DNA for subsequent analysis by next-generation sequencing. (B) Candidate genes identified by the CRISPR-Cas9 screen. Data analysis was performed by using the MAGeCK software suite (28) to identify enriched sgRNA, and the corresponding genes were rank ordered by robust rank aggregation (RRA) scores. Low RRA scores indicate a stronger selection of the corresponding gene.

member 3 (*OR5P3*) and pleckstrin homology domain-containing S1 (*PLEKHS1*) genes were also identified in the CRISPR-Cas9 screen.

PAPST1 is required for SBV attachment and entry. To validate the role of PAPST1 in SBV infection, we generated single-*SCL35B2*-knockout (KO) 293T cell clones, designated TKO1 and TKO2, by a CRISPR-Cas9 approach using two different sgRNAs. In comparison to control 293T (TCtrl) cells, TKO1 and TKO2 showed markedly reduced HS surface expression similar to that of heparinase II-treated cells (Fig. 2A and B). Intriguingly, both TKO1 and TKO2 were largely resistant to SBV infection, detected by viral Gc expression, compared to TCtrl cells, as shown by immunofluorescence (Fig. 2C) or flow cytometry (fluorescence-activated cell sorter [FACS]) analysis (Fig. 2D) at 24 h postinfection. In order to exclude potential bias due to cell culture adaptation of SBV BH80, we additionally investigated the HS dependency of two SBV isolates that were not further passaged on cell cultures after initial isolation. Similar to SBV BH80, both SBV isolates D512 and D495 infected TCtrl cells efficiently but were not able to infect TKO1 and TKO2 cells (Fig. 2I and J). To determine whether HS is essential for viral attachment, we quantified cell-bound SBV after inoculation for 1 h at 4°C by an S segment-based real-time quantitative PCR (RT-qPCR) assay. As shown in Fig. 2K (left), a pronounced reduction of cell surface-associated SBV RNA could be detected on TKO1 and TKO2 compared to TCtrl cells. Consistently, reduced levels of viral RNA were found in both TKO1 and TKO2 but not in TCtrl cells after incubation for 4 h at 37°C (Fig. 2K, right). Together, our findings suggest that PAPST1-triggered HS synthesis plays an important role in the binding of SBV to the cell surface and subsequent entry.

To confirm these findings in another SBV-susceptible cell type, we generated *SLC35B2* knockouts using human Huh7 cells. As described above for 293T cells, the two Huh7 knockout cell lines (HKO1 and HKO2) showed reduced HS surface levels compared to control cells (HCtrl) (Fig. 2E and F). In addition, the knockout of *SLC35B2* in Huh7 cells resulted in a significant degree of resistance to infection by SBV (Fig. 2G and H) although to a lesser extent than observed in the *SLC35B2* knockout 293T cells (Fig. 2C and D).

In order to validate these findings, we reintroduced SLC35B2 in the 293T knockout cell lines TKO1 (TKO1+LV-SLCB35B2) and TKO2 (TKO2-LV-SLC35B2) using lentiviral
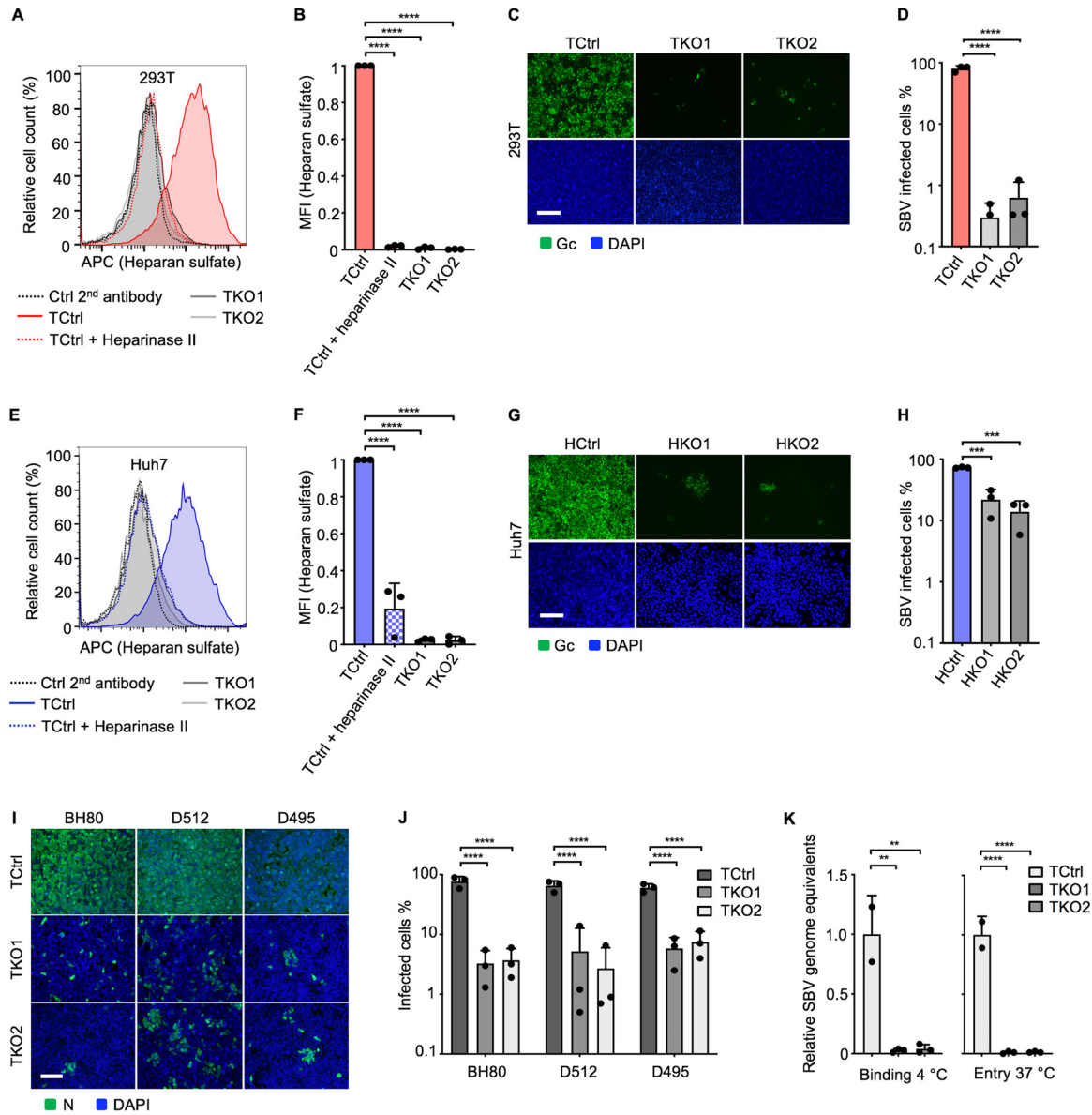
FIG 2 SLC35B2 is required for attachment and entry of SBV. (A) 293T (TCtrl) or *SLC35B2* KO (TKO1 and TKO2) cells were treated with or without heparinase II (4 U/ml) for 1 h at 37°C. Heparan sulfate (HS) surface staining of the cells was analyzed by FACS analysis using an anti-HS antibody (10E4). APC, allophycocyanin. (B) Graph summarizing the mean fluorescence intensity (MFI) of HS surface staining from three independent experiments as shown in panel A. Error bars indicate the standard deviations of data from three independent experiments. Statistical analyses were performed by one-way analysis of variance (ANOVA). Shown are means ± standard deviations. ****, $P < 0.0001$. (C) Fluorescence microscopy images of TCtrl, TKO1, and TKO2 cells infected with SBV (MOI of 0.1) for 24 h. Viral antigen was detected using an anti-SBV Gc-specific antibody. Nuclei were stained with DAPI (blue). Bar = 100 μm. (D) The 293T cell lines were infected with SBV (MOI of 0.1), for 24 h, fixed, and stained with an anti-SBV Gc-specific antibody. The frequency of SBV-infected cells was quantified by FACS analysis. Error bars indicate the standard deviations of data from three independent experiments. Statistical analyses were performed by one-way ANOVA. Shown are means ± standard deviations. ****, $P < 0.0001$. (E) HS surface staining of Huh7 cells as described above for panel A. (F) Quantification (MFI) of HS surface staining of the indicated Huh7 cells as described above for panel B. Error bars indicate the standard deviations of data from three independent experiments. Statistical analyses were performed by one-way ANOVA. Shown are means ± standard deviations. ****, $P < 0.0001$. (G) Fluorescence microscopy images of SBV-infected Huh7 cells as described above for panel C. (H) Quantification of SBV-infected Huh7 cells by FACS analysis as described above for panel D. Error bars indicate the standard deviations of data from three independent experiments. Statistical analyses were performed by one-way ANOVA. Shown are means ± standard deviations. ***, $P < 0.003$. (I) Fluorescence microscopy analysis of the indicated 293T cells infected with the SBV isolates BH80, D512, and D495 (MOI of 0.1) for 24 h. Infected cells were stained with an anti-SBV N-specific antibody (green). The nuclei were stained with DAPI (blue). Bar = 100 μm. (J) Quantification of the infected cells out of three independent experiments as shown in panel A by FACS analysis. Error bars indicate the standard deviations of data from three independent experiments. Two-way ANOVA was performed to determine the P values. ****, $P < 0.0001$. (K) RT-qPCR was performed to quantify cell surface-attached (left) or intracellular (right) SBV RNA. Cells were incubated with the virus at an MOI of 0.1 for 1 h at 4°C or for 4 h at 37°C, respectively. After several wash steps to remove unbound viral particles, RNA was extracted for RT-qPCR analysis. SBV RNA copy numbers were normalized to the mean values for TCtrl cells in each assay. Statistical analyses were performed by one-way ANOVA. Shown are means ± standard deviations. **, $P < 0.01$; ****, $P < 0.0001$.
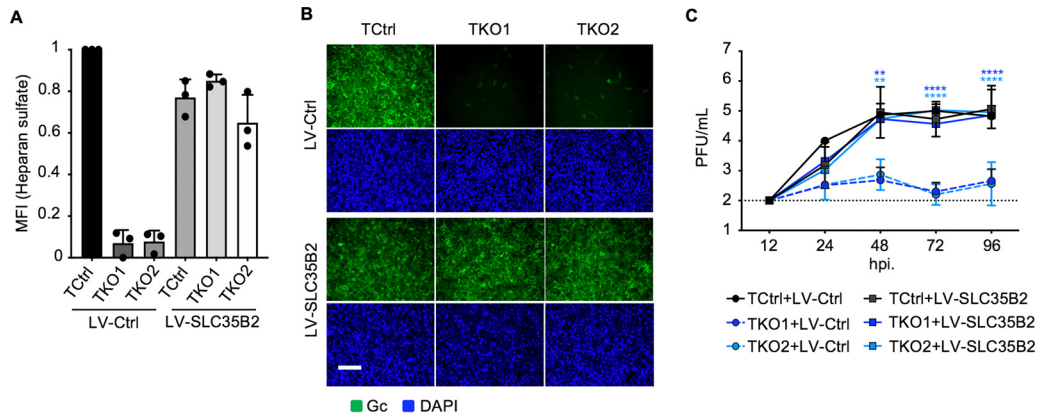
FIG 3 Reconstitution of SLC35B2 restores the infectivity of SBV. (A) HS staining (MFI) of 293T (TCtrl) and *SLC35B2* KO (TKO1 and TKO2) cells stably transduced with either a control lentivirus (LV-Ctrl) or an SLC35B2-encoding lentivirus (LV-SLC35B2) analyzed by FACS analysis. (B) Fluorescence microscopy of the indicated cell lines upon infection with SBV (MOI of 0.1) for 24 h. Viral antigen was detected using an anti-SBV Gc-specific antibody, and the nuclei were stained with DAPI. Bar = 100 μm. (C) SBV multiplication on the indicated cell lines upon infection with SBV (MOI of 0.001). At the indicated hours postinfection (hpi.), viral titers in the supernatants were determined by a plaque assay. Error bars indicate the standard deviations of data from three independent experiments. Two-way ANOVA was performed to determine the *P* values. **, $P < 0.005$; ****, $P < 0.0001$.

expression vectors (LV-SLC35B2). FACS analysis revealed that the expression of SLC35B2 in both knockout cell lines, TKO1+LV-SLCB35B2 and TKO2+LV-SLCB35B2, restored HS surface expression to levels comparable to those of 293T control cells (TCtrl cells transduced with an empty control vector [LV-Ctrl]) (Fig. 3A). In contrast, both TKO1 and TKO2 cells transduced with the control vector only, TKO+LV-Ctrl, did not restore HS surface expression (Fig. 3A). The reconstitution of *SLC35B2* in both TKO1 and TKO2 cells ablated the pronounced resistance to SBV infection, whereas control-transduced *SLC35B2* knockout cells remained resistant (Fig. 3B). Consistently, viral titers of up to 10^5 PFU/ml were observed in TKO1 and TKO2 cells reconstituted with SLC35B2 using an initial low infection dose of an MOI of 0.001, whereas only threshold levels were observed in control-transduced *SLC35B2* knockout cells (Fig. 3C). Collectively, our data suggest that in both 293T and Huh7 cells, *SLC35B2* is required for efficient SBV infection.

Heparan sulfate is required for infection by other bunyaviruses. Next, we investigated whether other bunyaviruses also require HS for efficient infection. We therefore infected TCtrl, TKO1, and TKO2 cells with LACV and RVFV, the latter expressing a green fluorescent protein (GFP) reporter gene. We additionally included herpes simplex virus 1 (HSV-1), which is known to enter cells by binding to HS (31, 32). Vesicular stomatitis virus (VSV) and influenza A virus (IAV), which are not dependent on HS for virus entry, served as controls (33, 34). As expected, HSV-1 only poorly infected *SLC35B2* knockout cells, whereas both VSV and IAV were able to infect control and knockout cells equally well (Fig. 4A and B). In contrast, the infection rates of *SLC35B2* knockout cells treated with RVFV or LACV were significantly reduced in TKO1 and TKO2 cells (Fig. 4A and B). To confirm that HS supports infection, we also inoculated heparinase II-treated 293T cells with SBV and LACV. Indeed, the number of cells infected with SBV and LACV decreased after treatment, whereas VSV infection was not affected (Fig. 4C). Altogether, *SLC35B2* expression and surface-resident HS are required to initiate infection by SBV and other bunyaviruses although to various degrees.

DISCUSSION

With genome-wide CRISPR-Cas9 screening, we identified the gene *SLC35B2*, encoding the sulfotransferase PAPST1, as a host cell attachment and entry factor for SBV. PAPST1 is involved in the synthesis of HS proteoglycan and the expression of cell surface HS (29). Accordingly, genetic ablation of *SLC35B2* and heparinase pretreatment of susceptible cells abrogate SBV replication and indicate the importance of HS for efficient host cell entry by several bunyaviruses. SLC35B2 might therefore represent a
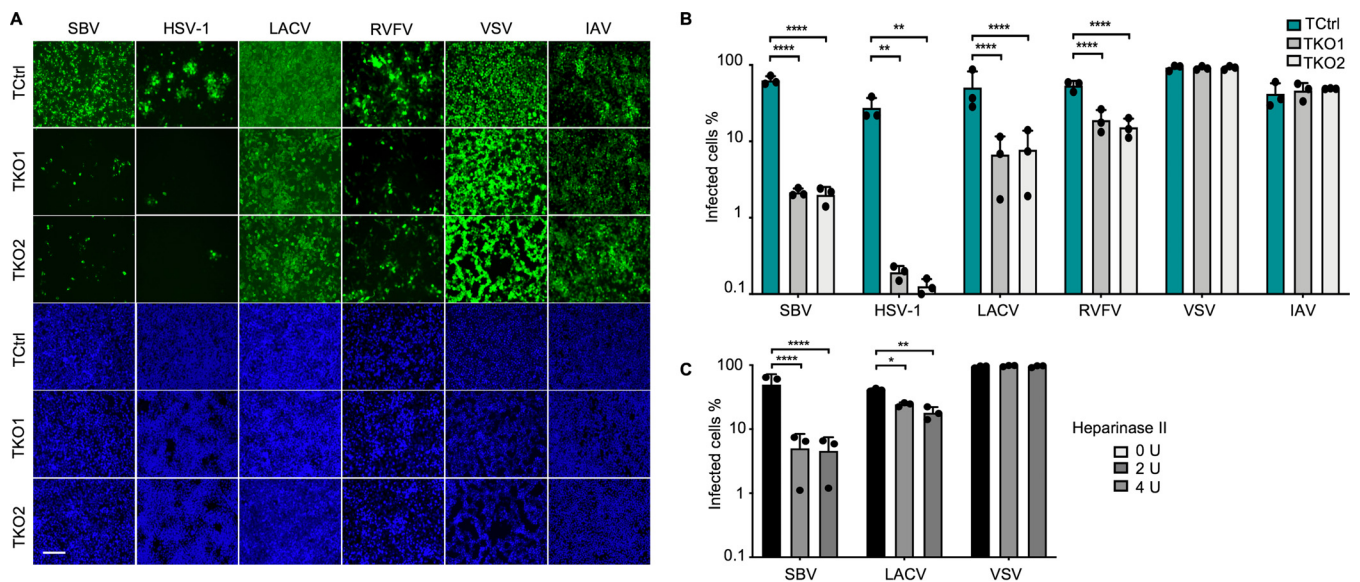
FIG 4 The presence of heparan sulfate enhances infection by SBV and other bunyaviruses, including LACV and RVFV. (A) Fluorescence microscopy analysis of the indicated 293T cells infected with SBV; LACV; or GFP-encoding HSV-1, RVFV, VSV, and IAV (MOI of 0.1) for 24 h. Infected cells were stained with an anti-SBV Gc antibody or an anti-LACV N-specific antibody or analyzed for GFP expression (green). The nuclei were stained with DAPI (blue). Bar = 100 μm. (B) Quantification of the infected cells out of three independent experiments as shown in panel A by FACS analysis. (C) FACS analysis of 293T cells treated with the indicated units per milliliter of heparinase II for 1 h at 37°C and then infected with SBV, LACV, or VSV-GFP for 2 h (MOI of 0.1). Error bars indicate the standard deviations of data from three independent experiments. Two-way ANOVA was performed to determine the P values. *, $P < 0.05$; **, $P < 0.005$; ****, $P < 0.0001$.

new target for the inhibition of this class of viruses. In addition to *SLC35B2*, other genes, such as *OR5P3* and *PLEKHS1*, were identified in the CRISPR-Cas9 screen; however, additional experiments are required to validate these hits.

Glycosaminoglycans (GAGs) such as HS are known to engage with attachment and entry of several viruses (32, 35–39). A previous study identified HS as a factor for the binding and cell entry of SBV and Akabane virus. The enzymatic removal of cell surface HS by heparinase treatment and targeted knockout of the EXT2 gene, encoding an enzyme, like PAPST1, involved in the HS biosynthesis pathway, resulted in significantly reduced infection rates (19). The *SLC35B2* gene detected by our CRISPR-Cas9 screening approach has previously been described to have an impact on HIV infection. However, in this case, the sulfation of a tyrosine residue on the CCR5 coreceptor of HIV-1 but not cell surface-resident HS was required for cell entry (21). For SBV, it is currently not known whether HS represents a general attachment factor or whether a specific protein at the cell surface needs to be sulfated to trigger SBV cell entry.

Previous knockout screens that showed the dependence of pathogen cell entry on HS identified multiple genes that were involved in HS biosynthesis (37, 40, 41), including xylosyltransferase, galactosyltransferase, or the exotosin (EXT) families of glycosyltransferases (42). However, our screen identified only the gene encoding the sulfotransferase PAPST1. This might suggest suboptimal conditions in our screening approach attributed to, e.g., the species of the original host, the choice of cell line, and long-term cell culture during multiple rounds of infection. These conditions possibly provoked a growth disadvantage of particular cell populations harboring specific gene knockouts that were then lost during cell passages. Accordingly, although loss-of-function CRISPR-Cas9 screenings are powerful tools to identify viral entry factors, this approach may have limitations, especially if these factors are essentially required for general host cell metabolism or if multiple entry factors exist.

The requirement of HS for efficient infection by RVFV has been described previously (36, 37), but we now demonstrate that the infectivity of SBV and LACV also depends on HS, highlighting the importance of this proteoglycan for viral cell entry by different bunyaviruses. Since the structures and architectures of the spike proteins of SBV and LACV are almost identical, we assume that Gc or the Gc/Gn heterodimer is responsible

for the binding of HS during the process of cell surface attachment of the virions (3, 43). However, for Bunyamwera virus, it has been shown that mutant viruses lacking the Gc head domain can still replicate in cell culture (44). Thus, the binding of Gc to HS is most likely not an exclusive factor mediating the cell entry of bunyaviruses, also indicating that the process of HS-dependent cell attachment and entry by SBV and other bunyaviruses is still not fully understood. Further research is therefore required, and the results presented here might serve as a solid basis for future research to elucidate the specific role of HS within this process and also for the *in vivo* situation.

MATERIALS AND METHODS

Cell lines. Human embryonic kidney 293T cells and African green monkey kidney Vero cells were purchased from the American Type Culture Collection (ATCC). Human hepatoma Huh7 cells were described previously (45). BHK-21 cells (CCLV 0164) were obtained from the Collection of Cell Lines in Veterinary Medicine, Biobank of the Friedrich-Loeffler-Institut, Insel Riems, Germany. All cell lines were maintained in Dulbecco's modified Eagle medium (DMEM) supplemented with fetal calf serum (FCS) (10%, vol/vol; Thermo Fisher Scientific) and penicillin-streptomycin (100 U/ml; Thermo Fisher Scientific) at 37°C with 5% CO_2.

CRISPR screen and Illumina sequencing and analysis. Genomic DNA (gDNA) of cell pellets was isolated using a Quick-DNA Miniprep Plus kit (Zymo Research). PCR was performed on gDNA to construct Illumina sequencing libraries, each containing 5 μg gDNA, according to the Broad Institute protocol for PCR of sgRNAs for Illumina sequencing and analysis using the MAGeCK software suite (28) as previously described (20).

Generation of knockout cell lines. *SLC35B2* KO cell clones were generated using CRISPR-Cas9-mediated genome editing via a lentiviral transduction system. We first generated 293T cells or Huh7 cell clones stably and highly expressing Cas9 (293T-Cas9 or Huh7-Cas9) by lentiviral transduction as described previously (20). The guide RNAs of oligonucleotides containing the *SLC35B2*-targeting sequences (NCBI RefSeq accession number NM_001286509.1), CCTGGCGCCCCGAACAGAGG and CACTCGGTTCATTAGCACC, and the control sgRNA sequence, AAAAAGCTTCCGCCTGATGG, were individually cloned into lentiGuide-Puro (Addgene plasmid 52963, a kind gift from Feng Zhang). Lentiviruses expressing sgRNA targeting *SLC35B2* and control sgRNA were produced as described previously (46). 293T-Cas9 or Huh7-Cas9 cells were transduced with the lentivirus and selected with puromycin at 1 μg/ml for 293T-Cas9 cells and 2 μg/ml for Huh7 cells after 2 days posttransduction. Single-cell clones were screened by FACS analysis for HS surface expression using an anti-heparan sulfate mouse monoclonal antibody (10E4 epitope) (catalog number 379225; Amsbio) followed by genotyping using specific primers for PCR (*SLC35B2* KO1 fwd [5′-CCAGCAGTCCAAACGGGATA-3′], *SLC35B2* KO2 fwd [5′-GGTGAAT CCAGACTTAGGAGGG-3′], and *SLC35B2* KO1-KO2 rev [5′-TGCTGACCCCAATGGAGATG-3′]).

Generation of SLC35B2-reconstituted 293T cell lines. A chemically synthesized *SLC35B2* gBlock (IDT) was amplified by PCR with specific primers (forward primer 5′-CGTGGATCCGCCGCCACCATG-3′ and reverse primer 5′-GCAGAATTCTCAAACTTTTTGC-3′). The PCR product was cloned into pLV-EF1a-IRES-Hygro (Addgene plasmid 85134) using BamHI and EcoRI restriction sites. Lentiviruses harboring *SLC35B2* or the pLV-EF1a-IRES-Hygro vector were produced in 293T cells as described previously (46). Control 293T (TCtrl) cells and *SCL35B2* knockout cell lines (TKO1 and TKO2) were transduced with either a lentivirus expressing SLC35B2 or an empty vector. The cells were then selected with 200 μg/ml hygromycin. Restored HS surface expression was confirmed by FACS analysis.

Heparan sulfate surface staining. Cells were detached with phosphate-buffered saline (PBS)–10 mM EDTA and resuspended in FACS buffer (PBS supplemented with 1% bovine serum albumin [BSA; Sigma-Aldrich]). Cells were washed three times with FACS buffer by centrifugation at 4,000 rpm for 2 min at 4°C, followed by resuspension of cell pellets. To stain for cell surface heparan sulfate, cells were incubated for 1 h at 4°C with an anti-heparan sulfate mouse monoclonal antibody (10E4 epitope) (catalog number 379225; Amsbio) (1:50 dilution). Cells were washed three times with FACS buffer as described above and subsequently stained with secondary goat anti-mouse Ig antibodies coupled to allophyco-cyanin (APC) (catalog number 550826; BD Pharmingen) (1:200). Samples were analyzed on a FACSCanto II system (BD). Typically, 2.0×10^4 cells were acquired, and APC intensities were examined. Data analysis was performed using FlowJo software v10.3.0.

Virus infections. Virus isolates SBV BH80/11-4 (SBV BH80), SBV D512/12 (SBV D512), and SBV D495/12-2 (SBV D495) were grown on BHK-21 cells for about 72 h and harvested by one cycle of freezing and thawing followed by centrifugation. Aliquots were stored at −80°C until further use. SBV isolates D512 and D495 were originally isolated in 2012 and kindly provided by Andreas Moss, Lebensmittel und Veterinärinstitut, Oldenburg, Germany. LACV was kindly provided by Ramasamy Raju, Meharry Medical College, Nashville, TN (47). The recombinant RVFV vaccine strain MP-12, generated to carry a green fluorescent protein (GFP) gene in place of the NSs gene, has been described previously (48). For infection with SBV isolates, RVFV, LACV, HSV1(17+)Lox-$_{pMCMV}$GFP (HSV-1) (49), or VSV (33), 293T or Huh7 cells were seeded in monolayers, infected with the viruses at the indicated MOIs (PFU per cell), and maintained in the infection medium DMEM supplemented with FCS (5%, vol/vol; Thermo Fisher Scientific) and penicillin-streptomycin (100 U/ml; Thermo Fisher Scientific). Infection with the IAV (A/SC35M) (H7N7) GFP reporter virus was performed as previously described (34).

(i) Immunofluorescence-based infection readout. At the indicated hours postinfection, cells were fixed using 4% paraformaldehyde (PFA) in PBS for 15 min, washed three times with PBS, and permeab-

ilized with 0.5% Triton X-100 in PBS for 5 min. Viral proteins were stained with antibodies against SBV isolates (anti-SBV Gc mouse monoclonal antibody [3] at 1:100 or anti-SBV N mouse monoclonal antibody [50] at 1:500) or LACV (anti-LACV N rabbit polyclonal antibody [kindly provided by Ramasamy Raju] at 1:1,000) for 1 h at room temperature. Next, cells were washed three times with PBS and stained using secondary antibodies (for SBV, anti-mouse IgG coupled to Alexa Fluor 488 [catalog number 115-546-062; Jackson ImmunoResearch]; for LACV, anti-rabbit Cy3-conjugated antibody [catalog number 711-165-152; Jackson ImmunoResearch]) for 1 h. Cells were washed, and nuclei were stained for 5 min using 4′,6-diamidino-2-phenylindole (DAPI) at a dilution of 1:5,000 in PBS. Finally, fluorescence images were acquired on a Zeiss Observer.Z1 inverted epifluorescence microscope (Carl Zeiss) equipped with an AxioCamMR3 camera using a 20× objective.

(ii) Flow cytometry-based infection readout. Briefly, cells were trypsinized and harvested by centrifugation at 4,000 rpm for 2 min at 4°C. Cells were fixed for 20 min on ice with BD Cytofix/Cytoperm fixation solution (BD Bioscience) followed by washing twice with BD Perm/Wash washing solution (BD Bioscience). Subsequently, samples were stained with primary antibodies (for SBV, anti-SBV Gc mouse monoclonal antibody at 1:100 or anti-SBV N mouse monoclonal antibody at 1:100; for LACV, anti-LACV N rabbit polyclonal antibody at 1:1,000; for RVFV, anti-RVFV rat antibody [51] at 1:200), followed by staining with secondary antibodies [for SBV, anti-mouse Ig antibodies coupled to APC (catalog number 550826; BD Pharmingen) at 1:200; for LACV, anti-rabbit IgG antibody coupled to BV421 (catalog number 565014; BD Pharmingen) at 1:200; for RVFV, anti-rat IgG(H+L) cross-absorbed antibody coupled to Alexa Fluor 488 (catalog number A11006; Life Technology) at 1:200]. Samples were analyzed on a FACSCanto II system (BD). The frequency of APC-, BV421-, Alexa Fluor 488-, or GFP-positive cells was quantified using FlowJo software v10.3.0.

Binding and entry assays. To determine the binding of viral particles at the cell surface, precooled cells were infected at an MOI of 0.1 for 1 h on ice. The supernatant was then removed, and the cells were washed 3 times with PBS to remove unbound virus particles. Cells were lysed with TRIzol reagent (Invitrogen), and after the addition of chloroform and phase separation, RNA was extracted from 100 μl of the aqueous layer using a KingFisher 96 Flex instrument (Thermo Scientific) and the NucleoMag Vet system (Macherey-Nagel) according to the manufacturers' instructions. RT-qPCR analysis was performed on a Bio-Rad CFX96 Touch real-time PCR detection system. A previously described, S segment-based RT-qPCR assay was used with an external standard for viral RNA quantification (52). To determine entry, cells were infected at an MOI of 0.1 and incubated at 37°C with 5% CO_2. At 4 h postinfection, cells were washed 3 times with PBS, and RNA extraction and RT-qPCR were performed as described above.

Determination of viral growth kinetics. Cells were inoculated with SBV at an MOI of 0.001 in infection medium as described above at 37°C for 1.5 h. Next, cells were washed twice with PBS, and the medium was replaced with infection medium. At 24, 48, 72, and 96 h postinfection, 150 μl of the supernatant was collected and subjected to a plaque assay for the determination of viral titers on Vero cells.

Heparinase treatment. Cells were seeded in 24-well plates 24 h prior to infection. The medium was removed, and cells were washed with DMEM with 0.2% BSA twice. Cells were then incubated with serial 2-fold dilutions of heparinase II (New England BioLabs) in DMEM with 0.2% BSA for 1 h at 37°C, followed by inoculation of SBV, LACV, or VSV at an MOI of 0.1 for 2 h at 37°C. The supernatant was then removed, and the cells were washed twice with DMEM with 5% (vol/vol) FCS before incubation for 24 h at 37°C. The frequency of infected cells was quantified by flow cytometry as described above.

REFERENCES

1. Hoffmann B, Scheuch M, Höper D, Jungblut R, Holsteg M, Schirrmeier H, Eschbaumer M, Goller KV, Wernike K, Fischer M, Breithaupt A, Mettenleiter TC, Beer M. 2012. Novel orthobunyavirus in cattle, Europe, 2011. Emerg Infect Dis 18:469–472. https://doi.org/10.3201/eid1803.111905.
2. De Regge N, Deblauwe I, De Deken R, Vantieghem P, Madder M, Geysen D, Smeets F, Losson B, van den Berg T, Cay AB. 2012. Detection of Schmallenberg virus in different Culicoides spp. by real-time RT-PCR. Transbound Emerg Dis 59:471–475. https://doi.org/10.1111/tbed.12000.
3. Hellert J, Aebischer A, Wernike K, Haouz A, Brocchi E, Reiche S, Guardado-Calvo P, Beer M, Rey FA. 2019. Orthobunyavirus spike architecture and recognition by neutralizing antibodies. Nat Commun 10:879. https://doi.org/10.1038/s41467-019-08832-8.
4. Beer M, Conraths FJ, Van Der Poel WHM. 2013. "Schmallenberg virus"—a novel orthobunyavirus emerging in Europe. Epidemiol Infect 141:1–8. https://doi.org/10.1017/S0950268812002245.
5. Wernike K, Conraths F, Zanella G, Granzow H, Gache K, Schirrmeier H, Valas S, Staubach C, Marianneau P, Kraatz F, Höreth-Böntgen D, Reimann I, Zientara S, Beer M. 2014. Schmallenberg virus—two years of experi-

ences. Prev Vet Med 116:423–434. https://doi.org/10.1016/j.prevetmed .2014.03.021.

6. Hughes HR, Adkins S, Alkhovskiy S, Beer M, Blair C, Calisher CH, Drebot M, Lambert AJ, de Souza WM, Marklewitz M, Nunes MRT, Shí X, ICTV Report Consortium. 2020. ICTV virus taxonomy profile: Peribunyaviridae. J Gen Virol 101:1–2. https://doi.org/10.1099/jgv.0.001365.

7. McJunkin JE, De Los Reyes EC, Irazuzta JE, Caceres MJ, Khan RR, Minnich LL, Fu KD, Lovett GD, Tsai T, Thompson A. 2001. La Crosse encephalitis in children. N Engl J Med 344:801–807. https://doi.org/ 10.1056/NEJM200103153441103.

8. Kruger DH, Figueiredo LTM, Song JW, Klempa B. 2015. Hantaviruses—globally emerging pathogens. J Clin Virol 64:128–136. https://doi.org/ 10.1016/j.jcv.2014.08.033.

9. Morrill JC, McClain DJ. 1996. Epidemiology and pathogenesis of Rift Valley fever and other phleboviruses, p 281–293. In Elliott RM (ed), The Bunyaviridae. The viruses. Springer, Boston, MA.

10. Ergönül Ö, Zeller H, Kiliç S, Kutlu S, Kutlu M, Cavusoglu S, Esen B, Dokuzoğuz B. 2006. Zoonotic infections among veterinarians in Turkey: Crimean-Congo hemorrhagic fever and beyond. Int J Infect Dis 10: 465–469. https://doi.org/10.1016/j.ijid.2006.06.005.

11. Zhang Y-Z, He Y-W, Dai Y-A, Xiong Y, Zheng H, Zhou D-J, Li J, Sun Q, Luo X-L, Cheng Y-L, Qin X-C, Tian J-H, Chen X-P, Yu B, Jin D, Guo W-P, Li W, Wang W, Peng J-S, Zhang G-B, Zhang S, Chen X-M, Wang Y, Li M-H, Li Z, Lu S, Ye C, De Jong MD, Xu J. 2012. Hemorrhagic fever caused by a novel bunyavirus in China: pathogenesis and correlates of fatal outcome. Clin Infect Dis 54:527–533. https://doi.org/10.1093/cid/cir804.

12. Elliott RM. 2014. Orthobunyaviruses: recent genetic and structural insights. Nat Rev Microbiol 12:673–685. https://doi.org/10.1038/ nrmicro3332.

13. Van Knippenberg I, Carlton-Smith C, Elliott RM. 2010. The N-terminus of Bunyamwera orthobunyavirus NSs protein is essential for interferon antagonism. J Gen Virol 91:2002–2006. https://doi.org/10.1099/ vir.0.021774-0.

14. Garry CE, Garry RF. 2004. Proteomics computational analyses suggest that the carboxyl terminal glycoproteins of bunyaviruses are class II viral fusion protein (beta-penetrenes). Theor Biol Med Model 1:10. https://doi .org/10.1186/1742-4682-1-10.

15. Hacker JK, Volkman LE, Hardy JL. 1995. Requirement for the G1 protein of California encephalitis virus in infection in vitro and in vivo. Virology 206:945–953. https://doi.org/10.1006/viro.1995.1017.

16. Kingsford L, Ishizawa LD, Hill DW. 1983. Biological activities of monoclonal antibodies reactive with antigenic sites mapped on the G1 glycoprotein of La Crosse virus. Virology 129:443–455. https://doi.org/10 .1016/0042-6822(83)90182-4.

17. Sundin DR, Beaty BJ, Nathanson N, Gonzalez-Scarano F. 1987. A G1 glycoprotein epitope of La Crosse virus: a determinant of infection of Aedes triseriatus. Science 235:591–593. https://doi.org/10.1126/science .3810159.

18. Ludwig GV, Israel BA, Christensen BM, Yuill TM, Schultz KT. 1991. Role of La Crosse virus glycoproteins in attachment of virus to host cells. Virology 181:564–571. https://doi.org/10.1016/0042-6822(91)90889-j.

19. Murakami S, Takenaka-Uema A, Kobayashi T, Kato K, Shimojima M, Palmarini M, Horimoto T. 2017. Heparan sulfate proteoglycan is an important attachment factor for cell entry of Akabane and Schmallenberg viruses. J Virol 91:e00503-17. https://doi.org/10.1128/JVI.00503-17.

20. Karakus U, Thamamongood T, Ciminski K, Ran W, Günther SC, Pohl MO, Eletto D, Jeney C, Hoffmann D, Reiche S, Schinköthe J, Ulrich R, Wiener J, Hayes MGB, Chang MW, Hunziker A, Yángüez E, Aydillo T, Krammer F, Oderbolz J, Meier M, Oxenius A, Halenius A, Zimmer G, Benner C, Hale BG, García-Sastre A, Beer M, Schwemmle M, Stertz A. 2019. MHC class II proteins mediate cross-species entry of bat influenza viruses. Nature 567:109–112. https://doi.org/10.1038/s41586-019-0955-3.

21. Park RJ, Wang T, Koundakjian D, Hultquist JF, Lamothe-Molina P, Monel B, Schumann K, Yu H, Krupzcak KM, Garcia-Beltran W, Piechocka-Trocha A, Krogan NJ, Marson A, Sabatini DM, Lander ES, Hacohen N, Walker BD. 2017. A genome-wide CRISPR screen identifies a restricted set of HIV host dependency factors. Nat Genet 49:193–203. https://doi.org/10 .1038/ng.3741.

22. Zhang R, Kim AS, Fox JM, Nair S, Basore K, Klimstra WB, Rimkunas R, Fong RH, Lin H, Poddar S, Crowe JE, Doranz BJ, Fremont DH, Diamond MS. 2018. Mxra8 is a receptor for multiple arthritogenic alphaviruses. Nature 557:570–574. https://doi.org/10.1038/s41586-018-0121-3.

23. Dudek AM, Zabaleta N, Zinn E, Pillay S, Zengel J, Porter C, Franceschini JS, Estelien R, Carette JE, Zhou GL, Vandenberghe LH. 2020. GPR108 is a

24. Marceau CD, Puschnik AS, Majzoub K, Ooi YS, Brewer SM, Fuchs G, Swaminathan K, Mata MA, Elias JE, Sarnow P, Carette JE. 2016. Genetic dissection of Flaviviridae host factors through genome-scale CRISPR screens. Nature 535:159–163. https://doi.org/10.1038/nature18631.

25. Savidis G, McDougall WM, Meraner P, Perreira JM, Portmann JM, Trincucci G, John SP, Aker AM, Renzette N, Robbins DR, Guo Z, Green S, Kowalik TF, Brass AL. 2016. Identification of Zika virus and dengue virus dependency factors using functional genomics. Cell Rep 16:232–246. https://doi.org/10.1016/j.celrep.2016.06.028.

26. Li Y, Muffat J, Javed AO, Keys HR, Lungjangwa T, Bosch I, Khan M, Virgilio MC, Gehrke L, Sabatini DM, Jaenisch R. 2019. Genome-wide CRISPR screen for Zika virus resistance in human neural cells. Proc Natl Acad Sci U S A 116:9527–9532. https://doi.org/10.1073/pnas.1900867116.

27. Doench JG, Fusi N, Sullender M, Hegde M, Vaimberg EW, Donovan KF, Smith I, Tothova Z, Wilen C, Orchard R, Virgin HW, Listgarten J, Root DE. 2016. Optimized sgRNA design to maximize activity and minimize off-target effects of CRISPR-Cas9. Nat Biotechnol 34:184–191. https://doi .org/10.1038/nbt.3437.

28. Li W, Xu H, Xiao T, Cong L, Love MI, Zhang F, Irizarry RA, Liu JS, Brown M, Liu X. 2014. MAGeCK enables robust identification of essential genes from genome-scale CRISPR/Cas9 knockout screens. Genome Biol 15:554. https://doi.org/10.1186/s13059-014-0554-4.

29. Kamiyama S, Ichimiya T, Ikehara Y, Takase T, Fujimoto I, Suda T, Nakamori S, Nakamura M, Nakayama F, Irimura T, Nakanishi H, Watanabe M, Narimatsu H, Nishihara S. 2011. Expression and the role of 3′-phosphoadenosine 5′-phosphosulfate transporters in human colorectal carcinoma. Glycobiology 21:235–246. https://doi.org/10.1093/glycob/ cwq154.

30. Kamiyama S, Suda T, Ueda R, Suzuki M, Okubo R, Kikuchi N, Chiba Y, Goto S, Toyoda H, Saigo K, Watanabe M, Narimatsu H, Jigami Y, Nishihara S. 2003. Molecular cloning and identification of 3′-phosphoadenosine 5′-phosphosulfate transporter. J Biol Chem 278:25958–25963. https:// doi.org/10.1074/jbc.M302439200.

31. WuDunn D, Spear PG. 1989. Initial interaction of herpes simplex virus with cells is binding to heparan sulfate. J Virol 63:52–58. https://doi.org/ 10.1128/JVI.63.1.52-58.1989.

32. Shieh MT, WuDunn D, Montgomery RI, Esko JD, Spear PG. 1992. Cell surface receptors for herpes simplex virus are heparan sulfate proteoglycans. J Cell Biol 116:1273–1281. https://doi.org/10.1083/jcb.116.5.1273.

33. Zimmer G, Locher S, Rentsch MB, Halbherr SJ. 2014. Pseudotyping of vesicular stomatitis virus with the envelope glycoproteins of highly pathogenic avian influenza viruses. J Gen Virol 95:1634–1639. https:// doi.org/10.1099/vir.0.065201-0.

34. Reuther P, Göpfert K, Dudek AH, Heiner M, Herold S, Schwemmle M. 2015. Generation of a variety of stable influenza A reporter viruses by genetic engineering of the NS gene segment. Sci Rep 5:11346. https:// doi.org/10.1038/srep11346.

35. Gardner CL, Ebel GD, Ryman KD, Klimstra WB. 2011. Heparan sulfate binding by natural Eastern equine encephalitis viruses promotes neurovirulence. Proc Natl Acad Sci U S A 108:16026–16031. https://doi.org/10 .1073/pnas.1110617108.

36. de Boer SM, Kortekaas J, de Haan CAM, Rottier PJM, Moormann RJM, Bosch BJ. 2012. Heparan sulfate facilitates Rift Valley fever virus entry into the cell. J Virol 86:13767–13771. https://doi.org/10.1128/JVI .01364-12.

37. Riblett AM, Blomen VA, Jae LT, Altamura LA, Doms RW, Brummelkamp TR, Wojcechowskyj JA. 2016. A haploid genetic screen identifies heparan sulfate proteoglycans supporting Rift Valley fever virus infection. J Virol 90:1414–1423. https://doi.org/10.1128/JVI.02055-15.

38. de Haan CAM, Li Z, te Lintelo E, Bosch BJ, Haijema BJ, Rottier PJM. 2005. Murine coronavirus with an extended host range uses heparan sulfate as an entry receptor. J Virol 79:14451–14456. https://doi.org/10.1128/JVI.79 .22.14451-14456.2005.

39. Barth H, Schäfer C, Adah MI, Zhang F, Linhardt RJ, Toyoda H, Kinoshita-Toyoda A, Toida T, van Kuppevelt TH, Depla E, von Weizsäcker F, Blum HE, Baumert TF. 2003. Cellular binding of hepatitis C virus envelope glycoprotein E2 requires cell surface heparan sulfate. J Biol Chem 278: 41003–41012. https://doi.org/10.1074/jbc.M302267200.

40. Robinson-McCarthy LR, McCarthy KR, Raaben M, Piccinotti S, Nieuwenhuis J, Stubbs SH, Bakkers MJG, Whelan SPJ. 2018. Reconstruction of the cell entry pathway of an extinct virus. PLoS Pathog 14:e1007123. https:// doi.org/10.1371/journal.ppat.1007123.

highly conserved AAV entry factor. Mol Ther 28:367–381. https://doi.org/ 10.1016/j.ymthe.2019.11.005.

41. Rosmarin DM, Carette JE, Olive AJ, Starnbach MN, Brummelkamp TR, Ploegh HL. 2012. Attachment of Chlamydia trachomatis L2 to host cells requires sulfation. Proc Natl Acad Sci U S A 109:10059–10064. https://doi.org/10.1073/pnas.1120244109.
42. Carlsson P, Kjellén L. 2012. Heparin biosynthesis. Handb Exp Pharmacol 207:23–41. https://doi.org/10.1007/978-3-642-23056-1_2.
43. Bowden TA, Bitto D, McLees A, Yeromonahos C, Elliott RM, Huiskonen JT. 2013. Orthobunyavirus ultrastructure and the curious tripodal glycoprotein spike. PLoS Pathog 9:e1003374. https://doi.org/10.1371/journal.ppat.1003374.
44. Shi X, Goli J, Clark G, Brauburger K, Elliott RM. 2009. Functional analysis of the Bunyamwera orthobunyavirus Gc glycoprotein. J Gen Virol 90:2483–2492. https://doi.org/10.1099/vir.0.013540-0.
45. Lanford RE, Guerra B, Lee H, Averett DR, Pfeiffer B, Chavez D, Notvall L, Bigger C. 2003. Antiviral effect and virus-host interactions in response to alpha interferon, gamma interferon, poly(I)-poly(C), tumor necrosis factor alpha, and ribavirin in hepatitis C virus subgenomic replicons. J Virol 77:1092–1104. https://doi.org/10.1128/jvi.77.2.1092-1104.2003.
46. Shalem O, Sanjana NE, Hartenian E, Shi X, Scott DA, Mikkelsen TS, Heckl D, Ebert BL, Root DE, Doench JG, Zhang F. 2014. Genome-scale CRISPR-Cas9 knockout screening in human cells. Science 343:84–87. https://doi.org/10.1126/science.1247005.
47. Thompson WH, Kalfayan B, Anslow RO. 1965. Isolation of California encephalitis group virus from a fatal human illness. Am J Epidemiol 81:245–253. https://doi.org/10.1093/oxfordjournals.aje.a120512.
48. Habjan M, Penski N, Spiegel M, Weber F. 2008. T7 RNA polymerase-dependent and -independent systems for cDNA-based rescue of Rift Valley fever virus. J Gen Virol 89:2157–2166. https://doi.org/10.1099/vir.0.2008/002097-0.
49. Snijder B, Sacher R, Rämö P, Liberali P, Mench K, Wolfrum N, Burleigh L, Scott CC, Verheije MH, Mercer J, Moese S, Heger T, Theusner K, Jurgeit A, Lamparter D, Balistreri G, Schelhaas M, De Haan CAM, Marjomäki V, Hyypiä T, Rottier PJM, Sodeik B, Marsh M, Gruenberg J, Amara A, Greber U, Helenius A, Pelkmans L. 2012. Single-cell analysis of population context advances RNAi screening at multiple levels. Mol Syst Biol 8:579. https://doi.org/10.1038/msb.2012.9.
50. Wernike K, Brocchi E, Cordioli P, Sénéchal Y, Schelp C, Wegelt A, Aebischer A, Roman-Sosa G, Reimann I, Beer M. 2015. A novel panel of monoclonal antibodies against Schmallenberg virus nucleoprotein and glycoprotein Gc allows specific orthobunyavirus detection and reveals antigenic differences. Vet Res 46:27. https://doi.org/10.1186/s13567-015-0165-4.
51. Ritter M, Bouloy M, Vialat P, Janzen C, Haller O, Frese M. 2000. Resistance to Rift Valley fever virus in Rattus norvegicus: genetic variability within certain "inbred" strains. J Gen Virol 81:2683–2688. https://doi.org/10.1099/0022-1317-81-11-2683.
52. Bilk S, Schulze C, Fischer M, Beer M, Hlinak A, Hoffmann B. 2012. Organ distribution of Schmallenberg virus RNA in malformed newborns. Vet Microbiol 159:236–238. https://doi.org/10.1016/j.vetmic.2012.03.035.